Measurement Location Analysis for Information Embedded Power Systems

Tiffany L. Lakins and Chika O. Nwankpa
Electrical and Computer Engineering Department
Drexel University
Philadelphia, PA USA
Email: tll38@drexel.edu, con22@drexel.edu

***Abstract*—With the advent of various smart grid implementations, it has become feasible and perhaps suggested, to investigate the preferred location for measurement reference. The highest ranked reference would most accurately observe the power system status taking into account errors on indirect measurements. A process for this selection is presented in the work, where the effect of both network and power system perturbations such as measurement distortion and load change are analyzed to aid in the decision-making.**

Keywords—indirect measurements, measurement reference, vantage point

I. INTRODUCTION

Wide-spread popularity of information embedded power systems [1] (or smart grids) range from large scale transmission systems, to small scale residential renewable installations. (It should be noted, however, that although synchronized phasor measurement installations are on the rise [2], it remains that majority of measurements are unsynchronized). Concurrent with this rise in smart grid implementations, is also an unprecedented rise in and variety of measurement type, location and redundancy. Such diversity and quantity in the area of metering lends itself to revisiting some of the "tried and true" practices of power system operation and maintenance, in order to determine if any substantial improvements or recommendations can be made.

One such common practice that may be of interest to revisit is the concept of power system "vantage point", where the term is meant to describe the location of measurement reference. Historically, it is assumed that the direct measurements available at (and indirect measurements through) the electric location of the system operator (often the substation) are the best at describing the present state of the system. However, in the age of "big data" [3-4], the legitimacy of this assumption can and should be investigated. Since one of the main objectives in any power system is observability [5], an accurate and reliable means to monitor the status of a power system is crucial to quality assurance and system security.

Furthermore, in the case of steady state, or even power system and network perturbations such as faults, load change, and measurement distortion, the preferred vantage point for measurement analysis may not be at traditional locations such as substations. This is because the preferred vantage point would provide – at any status of the system – the "best view" of what is actually occurring. Additional analyses can also be done to identify measurement zones based on vantage point. It is our argument that these measurement zones can be used in a given application such as distribution modeling, in addition to determining which zone has the best "view" of other zones.

In the remainder of the paper, the methodology behind vantage point (and measurement zone) designations will be discussed (section II), then an implementation example and results will be discussed for a simple four bus teed test circuit (section III), finally discussion and conclusions will be presented on the proposed ranking process (Section IV).

II. METHODOLOGY

Recall, we used the term "vantage point" to describe the measurement reference location. The portion (number of buses) of the power system that can be adequately observed by a particular vantage point we'll refer to as a "vantage zone". In order to rank the choice of vantage point, parameters such as measurement type, accuracy, sensitivity, location and intensity of system perturbations, as well as zone size should be taken into consideration.

A. Preferred Vantage Point Candidates

From the aforementioned general description, a vantage point could be any node or bus in a power system. For larger power systems in particular, this general definition may lead to an overly large search space for the selection scheme. Some general guidelines can be followed to reduce the size of this search space. Using the objective of maximizing vantage zone size, strong vantage point candidates would be at locations with a high number of measurements and circuit connections that rather easily lend themselves to indirect measurements and thus covers a larger vantage zone. For example, a branching bus with a voltmeter as well as ammeters for each branch current would perhaps be a better vantage point candidate than a load bus off a radial feed with just a voltmeter. This is a topological-based guideline.

An additional or alternative guideline can also be dictated by defining a desired vantage zone, or zone criteria. In this way, the search space is reduced (or ranked) by characteristics such as proximity to zone edges and computational effort required to observe the zone. Using this approach, for example, a specific area in a system can be designated as a desired zone, and the accuracy of various points' detectability

This work was supported in part by the Office of Naval Research under Award Number ONR #N00014-14-1-0061 and ONR #N00014-13-1-0611.

can be studied.

For smaller power systems such search space reduction need not be employed. Additionally, for analyses with lax time constraints, an exhaustive search may be implemented for large power systems. However this may be easier to implement with a desired zone in mind, or even with a known zone's bus cardinality. For the purposes of this work, the former guideline of desired zone will be implemented.

B. Direct and Indirect Measurement Sets

We define a direct set – with respect to a vantage point – as all the direct measurements located at that node or bus. An example direct set can be seen in (1) for a vantage point at *n*, denoted VP_n. As aforementioned, we defined a vantage zone, as the portion of the power system to be detected. More specifically, we'll refer to the "measurement zone" as all the indirect measurements for a vantage point given the corresponding direct set. An example measurement zone is seen in (2), where each indirect measurement is denoted as such via an asterisk. (Indirect measurements are those attainable via the use of given direct measurements and circuit laws [6].) The "size" of a vantage zone will be represented by bus cardinality of the measurement zone set, in the case of (2) this zone size would be 3 since only measurements at buses: *n+1*, *n-1* and *n-2* appear in the set.

$$M_{DM}^{VP_n} = \{m_{V_n}, m_{I_n}, m_{Q_n}, \ldots\} \tag{1}$$

$$M_{IM}^{VP_n} = \{m_{V_{n+1}}^*, m_{P_{n+1}}^*, m_{Q_{n-1}}^*, m_{I_{n-2}}^*, m_{P_{n-2}}^*\} \tag{2}$$

For the purposes of this work, both direct and indirect measurements will be in the form of complex voltage and currents. These measurements in particular are becoming more common in use due to deployment of devices such as Phasor Measurement Units (PMU), which provides synchronized phasor electric quantities, even though this work does not assume the presence of such devices. This is unlike traditional measurements which are often magnitudes (no phase angle) from standard voltmeter, wattmeter and ammeters.

C. Performance Metric

The goal of the vantage point selection scheme, which will now be presented, is to rank vantage point candidates according to parameters such as accuracy, sensitivity/robustness, and zone size. In this work, the method for reducing multiple parameters of various type and unit into a single metric will be based on a "fitness function". The fitness function, pulled from genetic algorithms [7], is based on the Darwinian concept of survival of the fittest, where types of "people" are assigned fitness values based on attributes, and after many "generations" of "breeding" the only "person" remaining represents the optimal solution.

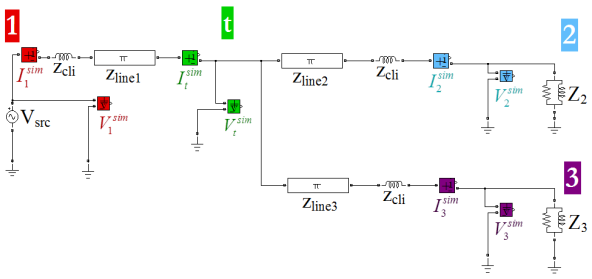

Fig. 1. MATLAB Simulink four bus teed test circuit with measurements

A fitness function mathematically speaking is simply a weighted sum, where the summands are the parameters to be optimized, and their corresponding weights represent each parameter's relative importance or contribution to overall fitness (the weight can and is used also as a scaling factor if raw parameter values span orders of magnitude). An example fitness function is seen in (3), where p1-p3 are the optimization parameters, while w1-w3 are their corresponding weights.

$$F = w1*p1 + w2*p2 + w3*p3 \tag{3}$$

For the purpose of this work, fitness will consider measurement errors.

D. Accuracy Quantization

Finally, to implement a selection scheme, we need a means to quantify the accuracy of the vantage point candidates. If given a desired zone (or zone measurements), the accuracy of a vantage point can be calculated through a multi-dimensional ABCD matrix implementation [8]. Recall that ABCD matrices of size [2x2] are often used in power systems analysis of transmission lines [9-10] (often called transmission matrices). Multi-dimensional ABCD matrix implementations are used in this particular application because it can be implemented with subsets of a systems voltage and current vectors, unlike full network matrices. As seen in (4), the dimension of the ABCD matrix can be altered to accommodate any size $[V_R\ I_R]^T$ (receiving end) or $[V_S\ I_S]^T$ (sending end) vector. This feature is non-existent in Y_{bus} or Z_{bus} matrix implementations since both require a vector of all system node voltages or currents. If the desired zone is represented as $[V_R\ I_R]^T$ pairs, and the vantage point candidates are represented as $[V_S\ I_S]^T$ pairs, then the known $[V_S\ I_S]^T$ vector (direct set) and calculated $[V_S\ I_S]^T$ vector can be compared to determine the accuracy of the ABCD transformation, as seen in (5) for phasor magnitudes. In the presence of $[V_R\ I_R]^T$ distortion and load/system changes, this comparison of known and calculated $[V_S\ I_S]^T$ can be used to quantify the accuracy of each vantage point's detection of the desired zone.

$$\begin{bmatrix} V_S^* \\ I_S^* \end{bmatrix} = \begin{bmatrix} A_{SR} & B_{SR} \\ C_{SR} & D_{SR} \end{bmatrix} * \begin{bmatrix} m_{V_R} \\ m_{I_R} \end{bmatrix} \tag{4}$$

$$\begin{bmatrix} |V_S^*|_{p.u.\ err} \\ |I_S^*|_{p.u.\ err} \end{bmatrix} = \begin{bmatrix} V_{base} & 0 \\ 0 & I_{base} \end{bmatrix}^{-1} * \left(\begin{bmatrix} |V_S^{sim}| \\ |I_S^{sim}| \end{bmatrix} - \begin{bmatrix} |V_S^*| \\ |I_S^*| \end{bmatrix} \right) \tag{5}$$

For the purposes of this work, it is assumed that the measurements of the sending end vector, denoted $[V_S^{sim}\ I_S^{sim}]^T$ in (5) is the benchmark value in comparison to indirect measurements of this vector.

III. Example and Results

The proposed methodology will now be employed on a simple four bus teed circuit (where a "teed" circuit is defined

by existence of a branching bus), as seen in Fig. 1. Defining a desired vantage zone of {2, 3}, (or measurement zone set of {V_2, I_2, V_3, I_3}) we will analyze and rank the two possible vantage points in the system: VP_1, and VP_t. The ranking will be based on the error of indirect measurements at these vantage point candidates as seen in (5).

A. Test Circuit and Simulation Environment

Test circuit seen in Fig. 1 was implemented in MATLAB Simulink software using SimPowerSystems toolbox, with circuit values shown in Table 1. The transmission lines: z_{line1}, z_{line2}, and z_{line3} are modeled as π line equivalent models with series impedance values of z_{ser1-3} and shunt admittances of y_{shunt}. The two loads: Z_2 and Z_3 are modeled as constant impedances. The voltage source, V_{src} is a 60Hz signal set to 120VRMS. S_{base} is 1kVA, and V_{base} is 120V; these were chosen based on a hardware setup in the Interconnected Power System Laboratory (IPSL) at Drexel University's Center for Electric Power Engineering. Inductors denoted 'z_{cli}' are also present in the circuit, and included to represent the current limiting inductors that are part of the emulated line hardware used in IPSL.

Simulink ideal measurements were placed to record the eight voltages and currents depicted in Fig. 1. These measurements were extracted using the "power_steadystate" MATLAB command. Both loads were varied from 10% to 300% of nominal impedance in 10% steps, resulting in 900 load combinations. Both load bus measurements were distorted with standard deviation values in the set: {1%, 5%, 10%, 30%}, resulting in 16 distortion combinations. In total, 14,400 distinct load /distortion combinations were generated.

Distortion was added to both measurement magnitude and angle as illustrated in (6) using the MATLAB normally distributed pseudorandom number generator, "randn". This command returned 5000 trials for each ε in the desired vantage zone to emulate a Gaussian white noise distribution. The output is initially normal Gaussian, thus scaling and shifting was implemented. Using the equation: X=μ + σ Z, where μ - the parameter's mean value, σ – its standard deviation, and Z - the standard normal distribution value, distortion effects were applied by a scaling of σ and shifting of μ to produce varied distortion levels around simulation measurement values.

$$\begin{bmatrix} m_{V_j} \\ m_{I_j} \end{bmatrix} = \begin{bmatrix} \left(\left|V_j^{sim}\right| + \varepsilon_{|V_j|}\right) \angle \left(\theta_{V_j^{sim}} + \varepsilon_{\theta_{V_j}}\right) \\ \left(\left|I_j^{sim}\right| + \varepsilon_{|I_j|}\right) \angle \left(\theta_{I_j^{sim}} + \varepsilon_{\theta_{I_j}}\right) \end{bmatrix} \quad (6)$$

B. Fitness Implementation

As aforemementioned, the implemented fitness will be a function of the errors seen in indirect measurements at the vantage point candidates. The fitness function used can be seen explicitly in (7), where, in reference to (3), w1-w3 all equal to 50, p1 is the reciprocal of the root mean square of the voltage magnitude per unit error, p2 is the reciprocal of the root mean square of current magnitude error, and p3 is the reciprocal of the root mean square error of complex power angle (power factor angle). It should be noted that (7) is an arbitrarily selected fitness function chosen only to incorporate dependancies on measurement type, accuracy, and sensitivity. The implementaion of equal weighting on the parameters is only an assumption, and for more informative fitness, sensitivity analyses of the parameters should be performed. Equal weighting could result in supressing otherwise revealing behavior.

$$F\{VP_n\} = 50 * \left(\frac{1}{RMS\left(\left|V_n\right|_{p.u.err}\right)}\right) + 50 * \left(\frac{1}{RMS\left(\left|I_n\right|_{p.u.err}\right)}\right) + 50 * \left(\frac{1}{RMS\left(\left|\theta_{S_n}\right|_{err}\right)}\right) \quad (7)$$

Recall, for every load/distortion combination, the specified intensity of Gaussian distortion was applied 5000 times to each measurement magnitude and angle. To determine the errors seen in (5), a multi-dimensional ABCD matrix was implemented of the form seen in (8). Distorted {V_2, I_2, V_3, I_3} measurements were used to calculate indirect measurements at the vantage points: VP_1, and VP_t for each distortion trial. Each vector of errors was reduced to a single value via root mean square calculation.

$$\begin{bmatrix} V_1^* \\ V_t^* \\ I_1^* \\ I_t^* \end{bmatrix} = \begin{bmatrix} \begin{bmatrix} a_{12} & a_{13} \\ a_{t2} & a_{t3} \end{bmatrix} & \begin{bmatrix} b_{12} & b_{13} \\ b_{t2} & b_{t3} \end{bmatrix} \\ \begin{bmatrix} c_{12} & c_{13} \\ c_{t2} & c_{t3} \end{bmatrix} & \begin{bmatrix} d_{12} & d_{13} \\ d_{t2} & d_{t3} \end{bmatrix} \end{bmatrix} * \begin{bmatrix} m_{V_2} \\ m_{V_3} \\ m_{I_2} \\ m_{I_3} \end{bmatrix} \quad (8)$$

C. Vantage Point Ranking

The fitness values for VP_1 and VP_t were generated for the aforementioned load and distortion combinations. Fig. 2 depicts a selected load variation of Z_2 while holding Z_3 at half of its nominal value. The presented results have 1% distortion applied. We see the shape of the fitness curves mimics that of the PV curve. From these results we see that across majority of the load settings, VP_t is the more "fit" vantage point, except for a brief crossover range near the point of voltage collapse of the PV curve. Fig. 2 also highlights the power corresponding to

TABLE I
SIMULATION CIRCUIT PARAMETERS

Parameter Name	Parameter Value
y_{shunt}	j94.25e-6 Ω^{-1}
z_{cli}	j5.43 Ω
z_{ser1}	0.13 + j2.17 Ω
z_{ser2}	0.12 + j0.59 Ω
z_{ser3}	0.16 + j1.10 Ω
Z_2^{nom}	34.88 + j2.02 Ω
Z_3^{nom}	79.91 + j2.65 Ω

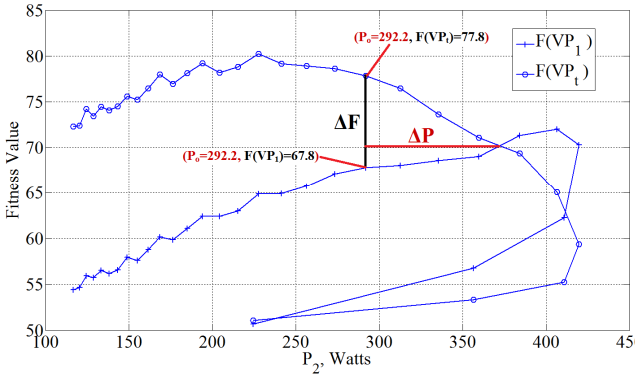

Fig. 2. Load Variation Results Depicting Possible Ranking Metrics

Z_2^{nom} (denoted P_0). Using this nominal power value; metrics can be introduced to aid in vantage point ranking and selection. Metrics such as power distance (denoted ΔP) to the crossover point or fitness distance (denoted ΔF) to alternative vantage (or crossover) point can be used in such a ranking/selection scheme.

The same fitness curves seen in Fig. 2 appear in Fig. 3 in the company of additional curves corresponding to Z_3 held at nominal and twice nominal impedance. Here again, all measurements are distorted at 1%. It is seen that the aforementioned crossovers still occur, however the duration of which decreases as Z_3 increases.

Fitness is again plotted for a few load and distortion variation cases in Fig. 4. In the displayed results, Z_3 is held constant at half nominal value, while Z_2 is varied. The distortion levels included all the permutations of 1% and 5% at vantage zone buses {2} and {3}. Displayed results show that an increase in distortion on either bus reduces the fitness at both vantage points. However VP_t reduces more than VP_1, resulting in very similar fitness across all loading levels. We also see increase in crossover duration, as well as a shift in the crossover load values. This may be the result of a phenomenon analogous to resonance. With both loads at 5% distortion, we see that fitness is nearly constant across all presented load levels. In the case where only measurements at {3}, (denoted $m_{V_3I_3}$) are 5% distorted we see that the stable region of the PV curve reduces more than the unstable region of the curve, resulting in an increased fitness for the unstable voltage points. The recommendation for the case when there is no differentiation between vantage points is for the operator to choose the vantage point with the more accurate sensor.

IV. Discussion and Conclusions

Since the vantage point electrically closest to the desired measurement zone {V_2, I_2, V_3, I_3} is VP_t, it is assumed that this vantage point may be of highest rank in this test system. Results confirm this assumption, but only in the case of minimal distortion and stable voltage conditions. As load variation approaches the point of voltage collapse we saw VP_1 outrank VP_t for various crossover durations. Additionally, we saw as distortion increased, ranking of the two vantage points was nearly pointless due to their extreme closeness in fitness value.

The technique presented in this work has many applications. One such application is the ability to use this technique to qualify and quantify competing measurement references that may exist for a given power system. In addition, measurement selection that captures the effect of both plant and communication characteristics can be developed based on the presented fitness function and ranking metrics. Another application could be the monitoring of system stability, as well as vantage point sets for use in improved state estimation.

Of note are two points with regard to the scalability of the proposed method in cases of larger test circuits. First, even in larger systems the proposed method could still be implemented at a local level, or on a subset of system buses. Second, we are currently looking at larger measurement set cases.

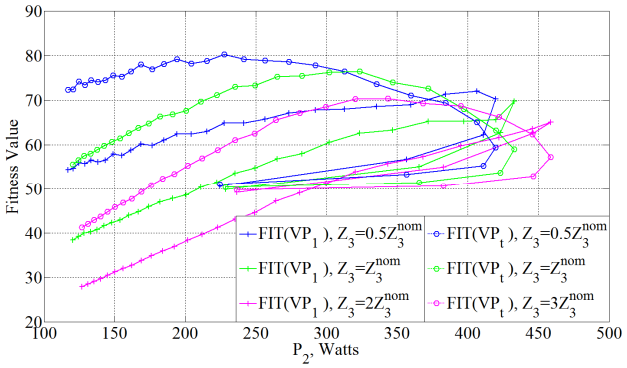

Fig. 3. Z_2 load variation results depicting effects Z_3 load settings, all measurements distorted at 1%.

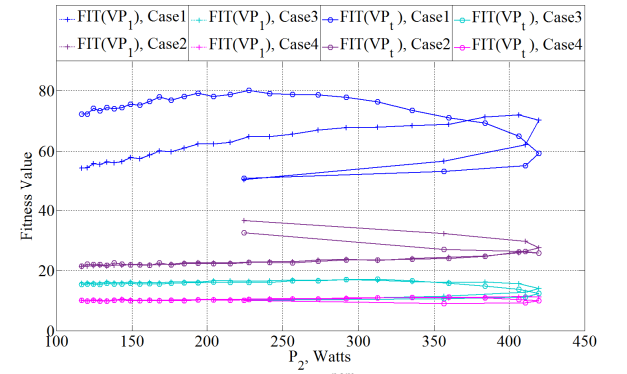

Fig. 4. Z_2 load variation results, Z_3=½ Z_3^{nom}, with measurement distortion levels as follows: {%$m_{V_2I_2}$, %$m_{V_3I_3}$}. Case 1: {1%, 1%}, Case 2: {1%, 5%}, Case 3: {5%, 1%}, Case 4: {5%, 5%}

References

[1] C.-H. Lo and N. Ansari, "The Progressive Smart Grid System from Both Power and Communications Aspects," *Communications Surveys & Tutorials, IEEE* , vol.14, no.3, pp.799,821, Third Quarter 2012.

[2] J. Liu et al., "Trade-Offs in PMU Deployment for State Estimation in Active Distribution Grids," *IEEE Trans. Smart Grid*, vol. 3, no. 2, pp. 915-924, Jun. 2012.

[3] M. Kezunovic et al, "The role of big data in improving power system operation and protection," *Bulk Power System Dynamics and Control - IX Optimization, Security and Control of the Emerging Power Grid (IREP), 2013 IREP Symposium* , vol., no., pp.1,9, 25-30 Aug. 2013.

[4] A. Ukil and R. Zivanovic, "Automated analysis of power systems disturbance records: Smart Grid big data perspective," *Innovative Smart Grid Technologies - Asia (ISGT Asia), 2014 IEEE*, vol., no., pp.126,131, 20-23 May 2014.

[5] T. L. Baldwin et al., "Power system observability with minimal phasor measurement placement," *IEEE Trans. Power Syst.*, vol. 8, no. 2, pp. 707-715, May 1993.

[6] I. Roytelman and S. M. Shahidehpour, "State estimation for electric power distribution systems in quasi real-time conditions," *IEEE Trans. Power Del.*, vol.8, no.4, pp.2009-2015, Oct. 1993.

[7] A. M. S. Zalzala and P. J. Fleming Eds., *Genetic Algorithms in Engineering Systems*. London, United Kingdom: The Institute of Electrical Engineers, 1997.

[8] A. A. Bhatti, "A computer based method for computing the N-dimensional generalized ABCD parameter matrices of N-dimensional systems with distributed parameters," *Twenty-Second Southeastern Symposium on System Theory, 1990*, pp. 590-593, 11-13 Mar 1990.

[9] J. D. Glover et al., "Transmission Lines: Steady-State Operation," in *Power System Analysis and Design, 4th* ed. Toronto, Ontario, Canada: Thomson Learning, 2008, ch. 5, sec. 1-3, pp. 235-250.

[10] A. R. Bergen and V. Vittal," Network Matrices" in *Power Systems Analysis, 2nd* ed. Englewood Cliffs, NJ: Prentice Hall, 2000, ch. 9, pp 294-319.